Proceeding of the 2004 American Control Conference
Boston, Massachusetts June 30 - July 2, 2004

Adaptive Force-Balancing Control of MEMS Gyroscope with Actuator Limits[1]

S. Jagannathan and Mohammed Hameed

Abstract – **This paper presents an adaptive force-balancing control (AFBC) scheme with actuator limits for a MEMS Z-axis gyroscope. The purpose of the adaptive force-balancing control is to identify major fabrication imperfections so that they are properly compensated unlike the case of conventional force-balancing controlled gyroscope. The proposed AFBC scheme controls the vibratory modes of the proof mass while ensuring that the control input satisfies the magnitude constraints and the performance of the gyroscope is enhanced in the presence of fabrication uncertainties. Consequently, commonly reported problems of MEMS gyroscope such as quadrature compensation, drive and sense axes frequency tuning are not needed and closed-loop identification of the angular rate is now possible without measuring the input/output phase difference. The proposed scheme also compensates the cross-damping terms that cause the zero-rate output (ZRO). Simulation results justify theoretical conclusions.**

I. INTRODUCTION

Micro machined gyroscope, which is one of the micro machined inertial sensors, has engrossed a lot of attention during the past few years for several applications. These are used for measuring rate or angle of rotation. Micromachining can contract the sensor size by orders of magnitude, reduce the fabrication cost significantly and allow the electronics to be integrated on the same silicon chip. Most of the MEMS gyroscopes are vibratory rate gyroscopes that have structures fabricated on crystal silicon or a polysilicon. The main mechanical component is a two degree-of-freedom vibrating structure, which is capable of oscillating in two directions in a plane. It's operating physics is based on the Coriolis effect. When a gyroscope is subjected to an angular velocity, the Coriolis effect transfers energy from one vibrating mode to another. The response of the second vibrating mode provides the information about the applied angular velocity [3].

Ideally in a conventional mode of operation of the gyroscope, the vibration modes are supposed to remain mechanically un-coupled, their natural frequencies should be matched and its output should only be sensitive to angular velocity. However, fabrication imperfections and environment variations cause the frequency of oscillation mismatch between the vibrating modes and a coupling between them through-off diagonal terms in the damping and the stiffness matrices. Thus, these imperfections abase the gyroscope performance and can cause false outputs unless a suitable AFBC scheme is used.

Therefore, several AFBC schemes [3,8] are proposed to cancel the effect of off-diagonal terms in the stiffness matrix (referred to as quadrature error) and to enhance the dynamic range of gyroscope. They rely on the exact measurement of input/output phase difference while they are sensitive to fabrication imperfections which are modeled as cross-damping terms resulting in zero-rate output (ZRO). Moreover, no magnitude constraints on the control input are asserted on the available adaptive force-balancing control schemes [1-9] and hence the practical viability of such schemes remains uncertain.

In this paper, a novel filtered error-based AFBC scheme for a MEMS Z-axis gyroscope is proposed. This algorithm provides an accurate estimation of the angular rate without measuring input/output phase difference as well as it identifies and compensates the cross-damping terms, which produce ZRO. Consequently, quadrature error compensation and drive and sense axis tuning is not required. Moreover, physical limitations dictate that hard limits be imposed on the magnitude of the control input to avoid damage to or deterioration of the system. This nonlinearity, represented as input saturation [11], in turn mandates that any control design must accommodate this constraint without sacrificing the performance. Since the available AFBC schemes [1-9] do not address the magnitude constraints, the proposed scheme is designed such that it can accommodate the actuator saturation effects. Closed loop performance is proven using Lyapunov analysis and in the presence of such constraints on the input.

[1] The authors are with the Department of Electrical and Computer Engineering and the Intelligent Systems Center, The University of Missouri-Rolla, 1870 Miner Circle, Rolla, MO 65401. Contact author's email address: sarangap@umr.edu.
Research supported in part by a NSF grant ECS #0296191 and the Intelligent Systems Center.

II. DYNAMICS OF MEMS GYROSCOPES

A typical MEMS vibratory gyroscope configuration includes a proof mass suspended by a spring, an electrostatic actuation and sensing mechanisms for forcing an oscillatory motion and sensing the position and velocity of the proof mass respectively. Assuming that the motion of the proof mass is constrained to be only along the x-y plane by taking the spring stiffness in the z-direction much larger than in the x and y directions, the measured angular rate is almost constant over a longer time interval, and linear accelerations are cancelled out, either as an offset from the output response or by applying counter-control forces, then the equations of motion of a gyroscope in simplified form is expressed as

$$m\ddot{x} + d_1\dot{x} + (k_1 - m(\Omega^2{}_y + \Omega^2{}_z))x + m\Omega_x\Omega_y y = \tau_x + 2m\Omega_z\dot{y}$$

$$m\ddot{y} + d_2\dot{y} + (k_2 - m(\Omega^2{}_x + \Omega^2{}_z))y + m\Omega_x\Omega_y x = \tau_y + 2m\Omega_z\dot{x} \quad (1)$$

where x and y are the coordinates of the proof mass relative to the gyroscope frame, k_1, k_2, d_1 and d_2 are the damping and spring coefficients, Ω_x, Ω_y and Ω_z are the angular velocity components along each axis of the gyro frame and τ_x, τ_y are the control forces. As seen from the equation (1), the last two terms $2m\Omega_z\dot{x}$ and $2m\Omega_z\dot{y}$ are due to the Coriolis forces, which are in turn used to measure the angular rate Ω_z. Clearly in an ideal z-axis MEMS gyroscope, only the component of angular rate along the z-axis Ω_z causes a dynamic coupling between the x and y axes because of the absence of stiffness and damping terms and due to the assumption that $\Omega^2{}_x \approx \Omega^2{}_y \approx \Omega_x\Omega_y \approx 0$. In practice, however, fabrication imperfections always occur, and cause the dynamic coupling between the x and y axes through the asymmetric spring and damping terms. These factors degrade the performance of MEMS gyroscopes. Thus taking into account the fabrication imperfections, the off-diagonal terms $d_{xy}\dot{x}$, $d_{xy}\dot{y}$, $k_{xy}x$ and $k_{xy}y$ are included in the dynamics (2.1) and (2.2) [14]. With the assumption $\Omega^2{}_x \approx \Omega^2{}_y \approx \Omega_x\Omega_y \approx 0$, $d_{xx} = d_1$, $d_{yy} = d_2$, $k_{xx} = k_1$ and $k_{yy} = k_2$, the equations of the motion are now rewritten as

$$m\ddot{x} + d_{xx}\dot{x} + d_{xy}\dot{y} + k_{xx}x + k_{xy}y = \tau_x + 2m\Omega_z\dot{y}$$

$$m\ddot{y} + d_{xy}\dot{x} + d_{yy}\dot{y} + k_{xy}x + k_{yy}y = \tau_y + 2m\Omega_z\dot{x} \quad (2)$$

The fabrication imperfections contribute mainly to the asymmetric spring and damping terms i.e. k_{xy} and d_{xy}. Therefore these terms are unknown, but can be assumed to be small. Based on the reference mass m, length q_0 and natural resonant frequency w_0 the non-dimensionalisation of equation (2) can be expressed as follows

$$\ddot{y} + d_{xy}\dot{x} + \frac{w_y}{Q_y}\dot{y} + w_{xy}x + w_y^2 y = \tau_y - 2\Omega_z\dot{x}$$

$$\ddot{y} + d_{xy}\dot{x} + \frac{w_y}{Q_y}\dot{y} + w_{xy}x + w_y^2 y = \tau_y - 2\Omega_z\dot{x}. \quad (3)$$

where Q_x and Q_y are respectively the x and y axis quality factor $w_x = \sqrt{k_{xx}/(mw_0{}^2)}$,

$w_y = \sqrt{k_{yy}/(mw_0{}^2)}, w_{xy} = k_{xy}/(mw_0{}^2), d_{xy} \leftarrow d_{xy}/(mw_0), \Omega_z \leftarrow \Omega_z / w_0,$

$\tau_x \leftarrow \tau_x / (mw_0{}^2 q_0)$ and $\tau_y \leftarrow \tau_y / (mw_0{}^2 q_0)$.

The equations of motion of a gyroscope can be non-dimensionalized for the sake of numerical simulations. Non-dimensionalisation also provides unified mathematical formulations for a large variety of gyroscope designs. In this work, the controllers will be designed based on the non-dimensional equations.

III. IDEAL GYROSCOPE BEHAVIOR

In this section the need for a AFBC scheme is demonstrated by using the ideal behavior of a gyroscope. To understand the ideal gyroscope behavior, the response has to be studied by considering its dynamics given by

$$\ddot{q} + w_o{}^2 q = -2\Omega\dot{q} \quad (4)$$

where

$$q = [x \;\; y]^T \text{ and } \Omega = \begin{bmatrix} 0 & -\Omega_Z \\ \Omega_Z & 0 \end{bmatrix}. \quad (5)$$

The dynamics in equation (4) represent a two degree-of-freedom pure spring mass system, which is oscillating on a rotating frame with an angular rate $\Omega = \Omega_Z$. When no angular rate is present, depending on whether the initial displacement vector is parallel to the velocity vector or not, this ideal gyroscope will either oscillate along the straight line or along an ellipsoid trajectory respectively [7]. Ellipticity of the gyroscope trajectory is undesirable because it directly affects the measurements.

When the gyroscope is experiencing the rotation, line of oscillation precesses and causes transfer of energy between the two axes while conserving the total energy of the gyroscope. Define the energy and the angular momentum of the gyroscope as

$$E = \frac{1}{2}\left(\dot{q}^T\dot{q} + w_0 q^T q\right), \quad (6)$$

and

$$P = q^T S\dot{q}, \quad (7)$$

where $S = \begin{bmatrix} 0 & 1 \\ -1 & 0 \end{bmatrix}$. Note that the angular momentum is an appropriate measure of how much the motion of a gyroscope deviates from a straight-line motion, since P will be zero for a straight-line oscillation. Taking the time

derivative of energy and momentum, equations (5) and (6) can be written as

$$\dot{E} = \dot{q}^T \ddot{q} + w_0^2 \dot{q}^T q = \dot{q}^T(-w_0^2 q - 2\Omega\dot{q}) + w_0^2 \dot{q}^T q = 0 \qquad (8)$$
$$\dot{P} = \dot{q}^T S\dot{q} + q^T \ddot{q} = q^T S(-w_0^2 q - 2\Omega\dot{q}) = -2\Omega_z q^T \dot{q}$$

Thus, it is clear from the equation (8) that the Coriolis acceleration term causes precession, i.e., a change of momentum and there is no change in total energy. It is also clear that in the absence of any angular rate, angular momentum is also conserved. When Ω_Z is zero or if the displacement and the velocity vectors q and $\dot{q}$ are parallel, the oscillation will remain in a straight line. Thus it is possible to measure the angular rate by generating a control action such that angular momentum is not changed even in the presence of angular rate. However in non-ideal gyroscopes, due to the presence of damping terms and other fabrication imperfections, the total energy and the angular momentum is not conserved even when the angular rate is zero. Thus to measure the angular rate accurately in any application using a non-ideal MEMS gyroscope, an AFBC scheme is necessary to ensure that the trajectory of the proof mass is in a straight-line in the x-y plane so that the total energy is held constant and angular momentum converges to zero. The reference trajectory, which is required, can be defined using an ideal gyroscope behavior.

IV. CONTROL SCHEME DEVELOPMENT

Next, we present the generation of a reference trajectory and an adaptive control scheme of achieving the force-balancing action for a non-ideal gyroscope.

A. Filtered error-based Adaptive Control

Suppose a reference trajectory given in (11) is generated such that is satisfies the motion of an ideal gyroscope while it simultaneously keeps the angular momentum to zero, i.e.

$$\ddot{q}_d + w_0^2 q_d = 0, \qquad (9)$$
$$P = q_d^T S\dot{q}_d = 0, \qquad (10)$$

where $q_d = [x_d \quad y_d]^T$. One such reference trajectory is given by

$$q_d = [\cos\alpha\, X_0 \sin(w_0 t) \quad \sin\alpha\, X_0 \sin(w_0 t)^T] \qquad (11)$$

where α the slope angle of the straight-line trajectory as is measured from the x-axis in the x-y plane. Rewrite the non-dimensional gyroscope equation as

$$I\ddot{q} + D\dot{q} + Kq + 2\Omega\dot{q} = \tau \qquad (12)$$

$K = \begin{bmatrix} w_x^2 & w_{xy} \\ w_{xy} & w_y^2 \end{bmatrix}$. where $D = \begin{bmatrix} w_x / Q_x & d_{xy} \\ d_{yx} & w_y / Q_y \end{bmatrix}$ and

Now to design a force balancing scheme given the desired trajectory $q_d(t)$, the error e(t) is defined as

$$e(t) = q_d(t) - q(t) \qquad (13)$$

Assumption 1: The desired trajectory is assumed to be bounded such that $\|q_d(t)\| \le q_B$.

Define a filtered tracking error *r (t)* as

$$r(t) = \dot{e} + \lambda e, \qquad (14)$$

where $\lambda = \lambda^T$ is a positive definite matrix selected by the designer. Differentiating (14) and substituting (12) and (13) in (14) to get

$$I\dot{r} = 2\Omega(\dot{q}_d + \lambda e) + Kq + D\dot{q} + (\ddot{q}_d + \lambda\dot{e}) - 2\Omega r - \tau \qquad (15)$$

Equation (15) can be rewritten in terms of filtered tracking error as

$$I\dot{r} = f(x) + (\ddot{q}_d + \lambda\dot{e}) - \tau, \qquad (16)$$

where the gyroscope dynamics after simplification can be written as

$$f(x) = 2\Omega(\dot{q}) + kq + D\dot{q} \qquad (17)$$

The dynamics f(x) is further expressed as

$$f(x) = [2\dot{q} \quad q \quad \dot{q}] \begin{bmatrix} \Omega \\ K \\ D \end{bmatrix} = W^T(x)\phi \qquad (18)$$

where $W(x) = [2\dot{q} \quad q \quad \dot{q}]^T$ is the regression vector of known functions and $\phi = [\Omega \;\; K \;\; D]^T$ is the vector of unknown parameters. An estimate of the nonlinear dynamics can be generated as

$$\hat{f}(x) = W^T(x)\hat{\phi} \qquad (19)$$

where the unknown parameter vector $\hat{\phi} = [\hat{\Omega} \;\; \hat{K} \;\; \hat{D}]^T$. Then, a control law without any constraints is given by

$$\tau = \hat{f}(x) + (\ddot{q}_d + \lambda\dot{e}) + k_v r \qquad (20)$$

where k_v is another design parameter matrix of appropriate dimension. Substituting (19) and (20) in (16) yields

$$\begin{aligned} \dot{r} &= -k_v r + f(x) - \hat{f}(x), \\ &= -k_v r + W^T(x)\tilde{\phi}, \end{aligned} \qquad (21)$$

where $\tilde{\phi} = \phi - \hat{\phi}$, is the error in unknown parameters. In order to account for the magnitude constraints on the input, select $\Delta u = \tau - v$ or $\tau = v + \Delta u$ where v is given by

$$v = \hat{f}(x) + (\ddot{q}_d + \lambda\dot{e}) + k_v r. \qquad (22)$$

Now applying the magnitude constraints on the control input, we have

$$\begin{aligned} \tau &= v && for\,|v(t)| \le \tau_{\max} \\ &= \tau_{\max}\,\mathrm{sgn}(v(t)) && for\,|v(t)| > \tau_{\max} \end{aligned} \qquad (23)$$

Equation (21) now results in $\dot{r} = -k_v r + W^T(x)\tilde{\phi} + \Delta u$ where Δu is defined as a disturbance. In order to combat disturbance, define $\dot{e}_\Delta$ as

$$\dot{e}_{\Delta} = -k_v e_{\Delta} + \Delta u. \quad (24)$$

Now define

$$e_u = r - e_{\Delta}. \quad (25)$$

Differentiating (25) and substituting (24) in (25) to get

$$\dot{e}_u(t) = -k_v e_u(t) + W^T(x)\tilde{\phi}, \quad (26)$$

Recap the adaptive control scheme as

$$\tau = W^T(x)\hat{\phi} + (\ddot{q}_d + \lambda\dot{e}) + k_v r,$$

with the parameter update

$$\dot{\hat{\phi}} = \gamma^{-1} W^T(x) e_u. \quad (27)$$

where γ^{-1} is a tuning parameter matrix selected diagonal with positive elements. This adaptive controller manufactures and estimate $\hat{\phi}$ for the unknown parameter vector ϕ by dynamic tuning using (27), thus the controller has its own dynamics. It is important to note that the angular rate is one of the unknown parameters in the parameter vector, which is being estimated and therefore with the proposed adaptive scheme, there is no need to measure input/output phase difference. The performance of the proposed AFBC scheme is described by the following theorem.

B. Parameter Updates

Theorem 1: (Adaptive controller with PE): Suppose the desired trajectory $q_d(t)$ is bounded as per Assumption 1 and assume the linear-in-paramters assumption (18) holds and the unknown paramter vector ϕ is a constant. Then, using the control input (22) with magnitude constraints (23) and by using the adaptive parameter tuning given by (27), the error e_u goes to zero asymptotically and the paramter estimates $\hat{\phi}(t)$ are bounded. With an additional PE condition, $\hat{\phi}(t)$ converges to ϕ asymptotically.

Proof: -Select a Lyapunov function candidate

$$V = \frac{1}{2}(e_u^T e_u) + \frac{1}{2}(\tilde{\phi}^T \gamma \tilde{\phi}), \quad (28)$$

with γ a symmetric positive definite weighting matrix.

Differentiating (28) to get

$$\dot{V} = e_u^T \dot{e}_u + (\tilde{\phi}^T \gamma \dot{\tilde{\phi}}). \quad (29)$$

Hence substituting the error dynamics (26)

$$\dot{V} = -e_u^T k_v e_u + \left[\tilde{\phi}^T (e_u^T W^T(x) + \gamma\dot{\tilde{\phi}})\right]. \quad (30)$$

By selecting the parameter tuning law as $\dot{\hat{\phi}} = \gamma^{-1} W^T(x) e_u$ yields

$$\dot{V} = -e_u^T k_v e_u. \quad (31)$$

In view of the definition $\tilde{\phi} = \phi - \hat{\phi}$, and the assumption that ϕ is constant, the selection for $\dot{\tilde{\phi}}$ yields the tuning law, which is given by

$$\dot{\hat{\phi}} = \gamma^{-1} W^T(x) e_u. \quad (32)$$

Since V is positive definite and $\dot{V}$ is negative semi definite, both e_u and $\tilde{\phi}$ are bounded according to Lyapunov's theorem. Boundedness of the parameter estimate $\hat{\phi}$ follows from the fact that ϕ is bounded. To show e_u (t) goes to zero one must use Barbalat's Lemma [10] to show that $\dot{V}$ goes to zero with t. Hence e_u vanishes as t becomes large. To accomplish this, differentiate to obtain

$$\begin{aligned} \ddot{V} &= -2e_u^T k_v \dot{e}_u \\ &= -2e_u^T k_v(-k_v e_u + W^T(x)\tilde{\phi}). \end{aligned} \quad (33)$$

The right hand side is bounded and demonstrates the bounded ness of e_u and $\tilde{\phi}$. Therefore, $\ddot{V}$ is bounded implying that $\dot{V}$ is uniformly continuous and by Barbalat's Lemma, $\dot{V}$ goes to zeros with t. Therefore e_u vanishes as t becomes large.

Applying an additional PE condition, it can be shown that parameter error goes to zero so that $\hat{\phi}$ converges to ϕ [10]. So far we have been able to show the asymptotic convergence of e_u with the boundedness of $\tilde{\phi}$, $\hat{\phi}$ or the parameter convergence using the PE condition. To show the boundedness of r and e, use the equation $\dot{r} = -k_v r + W^T(x)\tilde{\phi} + \Delta u$ and the following cases have to be considered.

Case 1: $|v| \le \tau_{\max}$:-In the presence of PE condition, $u = v \Rightarrow \Delta u = 0$. Then $\dot{r} = -k_v r + W^T(x)\tilde{\phi}$. Applying the PE condition $\tilde{\phi} \to 0 \Rightarrow \dot{r} = -k_v r$ is a linear system with stable matrix and hence $r \to 0$ as $t \to \infty$.

Case 2:

$|v| \ge \tau_{\max}$, $\quad u - v = \Delta u \quad \Rightarrow u = \tau_{\max} Sgn(v(t)) + v$

The filter tracking error dynamics can be written as

$$\begin{aligned} \dot{r} &= -k_v r + W^T(x)\tilde{\phi} + \Delta u \\ &= -k_v r + W^T(x)\tilde{\phi} + \tau_{\max} Sgn(v(t)) + W^T(x)\hat{\phi} + (\ddot{q}_d + \lambda\dot{e}) + k_v r \\ &= W^T(x)\phi + \tau_{\max} Sgn(v(t)) + (\ddot{q}_d + \lambda\dot{e}) \end{aligned} \quad (34)$$

Replacing $\dot{r} = \ddot{e} + \lambda\dot{e}$ into (34)

$$\begin{aligned} \ddot{e} + \lambda\dot{e} &= W^T(x)\phi + \tau_{\max} Sgn(v(t)) + \ddot{q}_d + \lambda\dot{e} \\ \ddot{q}_d - \ddot{q} &= W^T(x)\phi + \tau_{\max} Sgn(v(t)) + \ddot{q}_d \\ \ddot{q} &= -(W^T(x)\phi + \tau_{\max} Sgn(v(t))) \end{aligned} \quad (35)$$

Expanding (35) and denoting $q = y_1$ and $\dot{q} = y_2$ to get

$$\frac{d}{dt}\begin{bmatrix} y_1 \\ y_2 \end{bmatrix} = \begin{bmatrix} 0 & 1 \\ -K & -2\Omega - D \end{bmatrix}\begin{bmatrix} y_1 \\ y_2 \end{bmatrix} + \begin{bmatrix} 0 \\ 1 \end{bmatrix}\tau_{\max} Sgn(v(t)) \quad (36)$$

where K, D are positive constants. Equation (36) is a stable linear system provided $|D| > |2\Omega|$ and driven by a bounded input $\tau_{\max} Sgn(v(t))$. Hence the states $q, \dot{q}$ are bounded and the tracking error r is bounded.

C. Parameter Updates without PE

For practical controls purposes the result of the theorem is good enough, since the tracking error *r(t)* is small. However, it is very difficult to verify or guarantee the PE condition. Hence the following theorem relaxes the PE condition.

Theorem 2: (No PE condition requirement).Consider the hypothesis presented in Theorem 1, with the parameter updates provided by

$$\dot{\hat{\phi}} = \gamma^{-1} W^T(x) e_u - \kappa\gamma^{-1} \| e_u \| \hat{\phi} \quad (37)$$

with $\gamma = \gamma^T > 0$ and $\kappa > 0$ a small design parameter, then the error e_u and parameter estimation error, $\tilde{\phi}$ (or equivalently) $\hat{\phi}$, are UUB.

Proof: Follow steps similar to Theorem 1.

V. SIMULATION RESULTS

A simulation study using the preliminary design data of the MIT- SOI MEMS gyroscope was conducted to evaluate the proposed scheme. The data for certain parameters are given in Table 1. For simulation purposes, we allowed $\pm 5\%$ parameter variations for the spring and damping coefficients and assumed $\pm 0.1\%$ magnitude of nominal damping coefficients for their off-diagonal terms. Key parameters of the gyroscope are selected as:

Table 1
Z-AXIS GYROSCOPE AND AFBC PARAMETERS

$m = 10^{-6} kg$	$\Omega_z = 1\ rad/\sec$	$w_0 = 314.15\, rad/\sec$
$k_{xx} = 2000\, N/m$	$k_{xy} = 0.1\%\ k_{xx}\ N/m$	$k_{yy} = 1000\, N/m$
$d_{xx} = 2x10^{-6}(N-\sec)/m$	$d_{xy} = 1\% d_{xx}(N-\sec)/m$	$d_{yy} = 2.34x10^{-6}(N-\sec)/$
$\lambda = 5$	$K_v = 2000 I_3$	$\gamma = 500 I_7$
$X_0 = 10^{-6} m$	$\alpha = \pi/4$	$U_{\max} = 0.2\mu N$

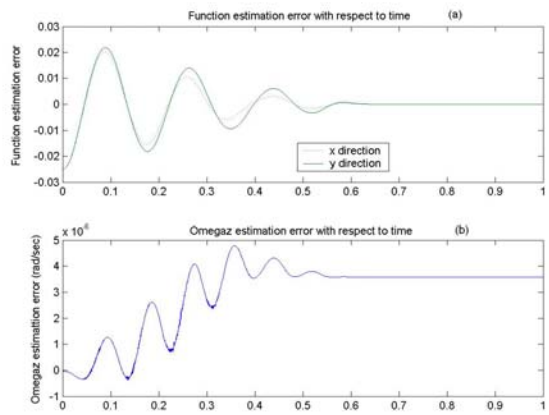

Fig. 1. Functional and rate estimation error.

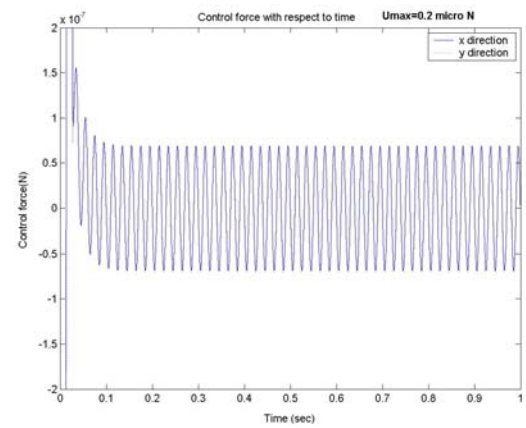

Fig 2. Control input with magnitude constraints.

Desired Trajectory is given by, $q_d = [X_0 \cos\alpha \sin w_0 t \quad X_0 \sin\alpha \cos w_0 t\ ]^T$. The actual and desired error, is plotted in micro meters and the control inputs are in micro Newton meter.

Figure 1 (a) shows that the function estimation error, f(x), converges to zero over time and the convergence happens within 1 second. Similarly, angular rate estimation error converges to zero very quickly as shown in Figure 1(b). The trajectory tracking error converges to zero with magnitude constraints on the input is illustrated in Figure 2. As displayed in Figure 3, large transients in the control input are observed when magnitude constraints are not used. Suitable limits will improve both transient and steady state tracking performance.

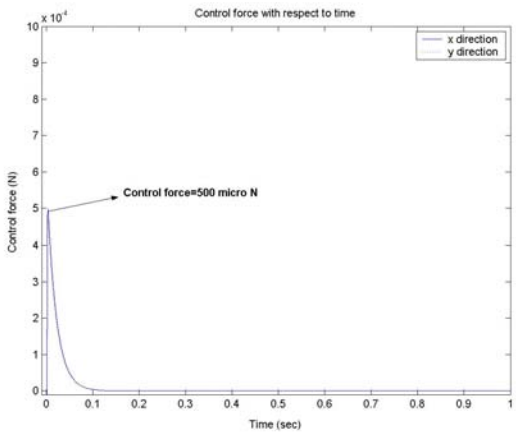

Fig 3. Control input without magnitude constraints**.**

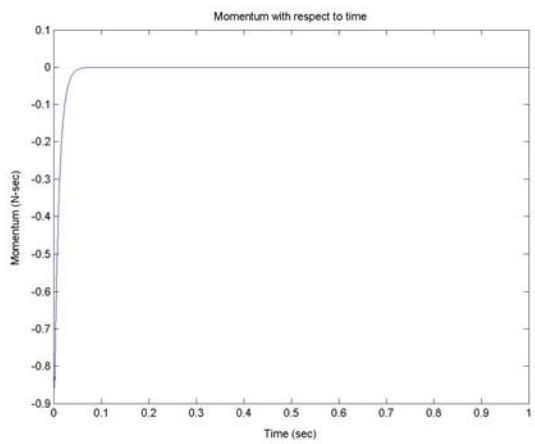

Fig. 4. Angular momentum over time.

Since the angular momentum of the gyroscope held at zero, as illustrated in Figure 4, the proof mass of the gyroscope converges in a straight line motion as displayed in Figure 5. From these results, the proposed AFBC scheme offers a superior performance.

VI. CONCLUSIONS

Past works on dynamic analysis of MEMS gyroscopes indicate that fabrication imperfections are a major limiting factor of the performance. Conventional force balancing control schemes do not provide sufficient excitation and as a result, all major fabrication imperfections cannot be identified and compensated. Furthermore magnitude constraints are not applied resulting in unwanted transients. Using the proposed AFBC schemes, additional richness of excitation is supplied to the gyroscope and thus quadrature compensation, drive and sense axis tuning, and closed-loop angular rate estimation is possible without ZRO. Simulation results using the MIT-SOI MEMS gyroscope data indicate the superior performance of the proposed scheme.

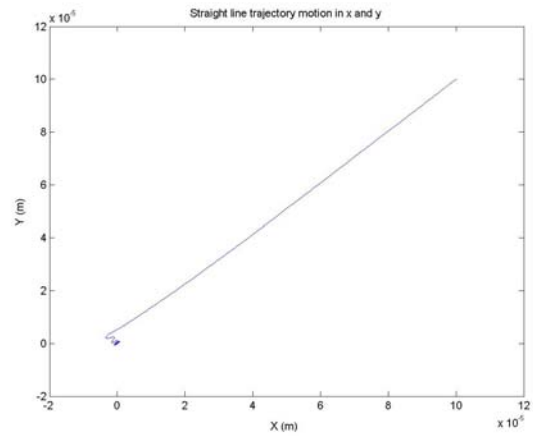

Fig. 5. Straight-line motion.

REFERENCES

[1] N. Yazdi, F. Ayazi and K. Najafi, "Micromachined inertial sensors," Proceedings of the IEEE, Vol. 86, August 1998, pp. 1640-1659.

[2] W. A. Clark, "Micromachined vibratory rate gyroscopes," Doctoral Thesis, Department of Mechanical Engineering, University of California, Berkeley, 1997.

[3] A. M. Shkel, R. Horowitz, A. A. Seshia, Sungsu Park and R. T. Howe. "Dynamics and control of micromachined gyroscope," Proceedings of the American Control Conference, Vol. 3, June 1999, pp. 2119-2124.

[4] P. B. Ljung, "Micromachined gyroscope with integrated electronics," Doctoral Thesis, Department of Electrical Engineering, University of California, Berkeley, 1997.

[5] A. Shkel, R. T. Howe, R. Horowitz, "Modeling and simulation of micromachined gyroscopes in the presence of imperfections," International Conference on Modeling and Simulation of Microsystems (MSM'99), pp. 605-608, Puerto Rico, U.S.A, April 1999.

[6] Robert P. Leland, "Lyapunov based adaptive control of a MEMS gyroscope," Proc. of the American Control Conference, Vol. 5, AK, May 2002, pp. 3765-3770.

[7] S. Park, R. Horowitz, "Adaptive control of the conventional mode of operation of MEMS gyroscopes," Journal of MEMS, Vol. 12, No. 1, Feb. 2003, pp. 101-108.

[8] C. Acar, S. Eler, A. M. Shkel, "Concept implementation and control of wide bandwidth MEMS gyroscope," Proc. of the American Control Conference, Vol. 2, Arlington, VA June 2001, pp. 1229-1234.

[9] Stephen D. Senturia, "Microsystems design," Kluwer Academic Publishers, 4th edition 2002.

[10] F. L. Lewis, S. Jagannathan and A. Yesildirek, "Neural network control of robot manipulators and non-linear systems," Taylor and Francis, 1999.

[11] S.P. Karason and A.M. Annaswamy "Adaptive control in presence of input constraints," IEEE Transactions on Automatic Control, Vol. 39, November 1994, pp. 2325-2330.